Journal of Physiology (1992), **457**, *pp.* 257–276
With 9 figures
Printed in Great Britain

A ROLE FOR LOW-FREQUENCY, RHYTHMIC SYNAPTIC POTENTIALS IN THE SYNCHRONIZATION OF CAT THALAMOCORTICAL CELLS

BY IVAN SOLTESZ* AND VINCENZO CRUNELLI†

From the Department of Visual Science, Institute of Ophthalmology, Judd Street, London

(*Received 17 December 1991*)

SUMMARY

1. Low-frequency, rhythmic synaptic potentials and their ability to evoke and modulate membrane potential oscillations in thalamocortical (TC) cells of the cat dorsal lateral geniculate nucleus (dLGN) were investigated using intracellular recordings in a brain slice preparation. Three types of rhythmic synaptic potentials were distinguished: EPSPs, IPSPs and 'complex synaptic potentials' consisting of an IPSP followed by an EPSP.

2. The frequency of all three types of synaptic potentials was insensitive to changes in the membrane potential. At potentials positive to −50 mV, the EPSPs and the complex potentials gave rise to action potentials, while between −65 and −80 mV all three types of synaptic potential evoked low-threshold Ca^{2+} potentials. TC cells which displayed rhythmic synaptic potentials were either cells that showed spontaneous pacemaker oscillation or cells that were brought to oscillate by the rhythmic EPSPs or depolarizing (i.e. reversed) IPSPs.

3. The low-frequency ($1{\cdot}9 \pm 0{\cdot}2$ Hz), rhythmic EPSPs were observed in 23 (out of 192) cells, were abolished by tetrodotoxin (TTX; $n = 4$) and by the combined application of DL-2-amino-5-phosphonovaleric acid and 6-cyano-7-nitroquinoxaline-2,3-dione ($n = 3$), and were insensitive to bicuculline ($n = 4$). Paired intracellular recordings ($n = 32$) demonstrated the presence of simultaneously occurring EPSPs in a pair of cells situated 75 μm apart.

4. The low-frequency ($2{\cdot}2 \pm 0{\cdot}3$ Hz), rhythmic IPSPs were observed in 5 (out of 192) cells, were blocked by bicuculline ($n = 3$), and reversed in polarity at −65 mV. The low-frequency ($1{\cdot}3 \pm 0{\cdot}3$ Hz), rhythmic 'complex potentials' were observed in 5 (out of 192) cells and were abolished by TTX ($n = 2$).

5. Intracellular depolarizing current pulses delivered at different phases of the pacemaker oscillations revealed the existence of two different types of phase resetting. Furthermore, a current pulse of critical amplitude and duration applied at a specific phase of the cycle abolished the pacemaker oscillations.

6. These results indicate that the low-frequency, rhythmic synaptic potentials

* To whom correspondence should be addressed at the Centre de Recherche en Neurobiologie, Hôpital de l'Enfant-Jésus, Université Laval, 18ème Rue, Québec, G1J 1Z4, Canada.

† Present address: Department of Physiology, University of Wales College of Cardiff, Museum Avenue, Cardiff CF1 1SS.

MS 9976

recorded in TC cells of the dLGN (i) originate from other TC cells that are in the pacemaker oscillating mode, (ii) are capable of driving other TC cells to oscillate rhythmically, or of modulating the frequency of pacemaker oscillations, and (iii) provide a means by which oscillatory activities of TC cells can be synchronized in the absence of sensory, cortical and reticular thalamic inputs.

INTRODUCTION

During the deep stages of synchronized sleep the EEG is characterized by δ-waves (0·5–4 Hz) (Hirsch, Fourment & Marc, 1983; Steriade, Jones & Llinas, 1990). Recent *in vivo* and *in vitro* studies have demonstrated the presence of membrane potential oscillations of similar frequencies in thalamocortical (TC) cells of various thalamic nuclei in different species (Crunelli, Kelly, Leresche & Pirchio, 1987*a*; McCormick & Prince, 1987; Leresche, Jassik-Gerschenfeld, Haby, Soltesz & Crunelli, 1990; McCormick & Pape, 1990*a*, *b*; Leresche, Lightowler, Soltesz, Jassik-Gerschenfeld & Crunelli, 1991; Soltesz, Lightowler, Leresche, Jassik-Gerschenfeld, Pollard & Crunelli, 1991; Steriade, Curró Dossi & Nunez, 1991*b*). In particular, the pacemaker oscillations, that occur when the membrane potential of TC cells is negative to -55 and positive to -80 mV, consist of rhythmic (0·5–4 Hz), large amplitude depolarizations (i.e. the low-threshold Ca^{2+} potentials) that often evoke a single or a high-frequency burst of action potentials (Leresche *et al.* 1990, 1991; McCormick & Pape, 1990*a*). These pacemaker oscillations have been shown to involve an interplay between the T-type Ca^{2+} current, I_T, (underlying the low-threshold Ca^{2+} potential) (Coulter, Huguenard & Prince, 1989; Crunelli, Lightowler & Pollard, 1989; Hernandez-Cruz & Pape, 1989; Suzuki & Rogawski, 1989), and the hyperpolarization-activated, mixed cation current, I_h (Pollard & Crunelli, 1988; McCormick & Pape, 1990*a*, *b*; Soltesz *et al.* 1991), and, since they are insensitive to tetrodotoxin (TTX), they represent spontaneous oscillations (Leresche *et al.* 1990, 1991).

TC cells that show the pacemaker oscillations (hereafter referred to as pacemaker cells) have to be synchronized for δ-waves to occur as a macroscopic EEG event. A possible synchronizing device could be the reticular thalamic nucleus, which is reciprocally connected to the majority of dorsal thalamic nuclei (Jones, 1985), and/or the corticothalamic loop (Steriade, Curró Dossi & Nunez, 1991*a*; Steriade *et al.* 1991*b*). As far as the dorsal lateral geniculate nucleus (dLGN) is concerned, an additional mechanism of synchronization might be via intrageniculate axon collaterals of TC cells. Although the number and importance of these collaterals is still a matter of controversy (Friedlander, Lin, Stanford & Sherman, 1981; Stanford, Friedlander & Sherman, 1983; Jones, 1985; Humphrey & Weller, 1988), their presence has been demonstrated by Golgi staining (Ramón y Cajal, 1911; O'Leary, 1940; Guillery, 1966; Scheibel & Scheibel, 1966; Tombol, 1967; Tombol, Madarasz, Hajdu, Somogyi & Gerle, 1978; Madarasz, Gerle, Hajdu, Somogyi & Tombol, 1978) and intracellular injection of horseradish peroxidase (HRP) (Friedlander *et al.* 1981; Stanford *et al.* 1983; Von Horn, Hamos & Sherman, 1986; Humphrey & Weller, 1988) or biocytin (S.M. Sherman, personal communication).

In this paper we report that low-frequency, rhythmic, excitatory postsynaptic potentials (EPSPs), inhibitory postsynaptic potentials (IPSPs) as well as IPSP–EPSP sequences ('complex potentials') occur in TC cells of the cat dLGN recorded

in slices that did not contain the perigeniculate nucleus. It is suggested that they originate from pacemaker neurones via intranuclear axon collaterals. TC cells which display these rhythmic potentials can be either pacemaker cells or they only exhibit membrane potential oscillations that are driven by the rhythmic synaptic potentials. In addition, experiments performed with intracellular current pulses, designed to mimic EPSPs or depolarizing (i.e. reversed) IPSPs, revealed two different types of phase resetting mechanisms in the pacemaker oscillations, and showed the existence of a singularity, demonstrating the non-linear nature of interactions which take place between neuronal oscillators in the dLGN. A preliminary report of some of the results described in this paper has been published (Soltesz & Crunelli, 1991).

METHODS

The preparation of cat dLGN slices has been described previously (Crunelli, Leresche & Parnavelas, 1987*b*; Leresche *et al.* 1991). Briefly, male and female cats (1·0–3·5 kg) were anaesthetized (2:1, O_2: N_2, 1·2% halothane) and a block of tissue containing the LGN was separated from the rest of the brain by two cuts made parallel to the plane of the optic tract. The animals were killed by a coronal cut at the level of the inferior colliculus to free the brain from the spinal cord and brain stem. Slices of the dLGN (300–400 μm) were prepared from this tissue block using a Vibroslice (Campden Instruments), and in most of the experiments the whole of lamina A was removed to ensure that the perigeniculate nucleus was not present in the slice. The slices were then transferred to a recording chamber and perfused with a warmed (35 ± 1 °C), continuously oxygenated (95% O_2, 5% CO_2) medium of composition (mM): NaCl, 134; KCl, 3·25; KH_2PO_4, 1·25; $MgSO_4$, 0·5–1·0; CaCl, 2·5; $NaHCO_3$, 16; and glucose, 10.

Impaled neurones in the dLGN were identified as TC cells by their location in the slice and by the presence of a low-threshold Ca^{2+} potential and of a depolarizing 'sag' in their voltage response to a pulse of hyperpolarizing current (Jahnsen & Llinas, 1984; Crunelli *et al.* 1987*b*; McCormick & Pape, 1988). Intracellular glass microelectrodes were filled with 1 M potassium acetate, and voltage and current records were stored on a Racal 4D tape recorder or a Biologic DAT recorder for subsequent analyses. The antagonists used in this study were dissolved in the perfusion medium.

Drugs were obtained from the following sources: TTX and bicuculline methiodide from Sigma; DL-2-amino-5-phosphonovaleric acid (APV) and 6-cyano-7-nitroquinoxaline-2,3-dione (CNQX) from Tocris Neuramin. All quantitative data are expressed in the text as the mean ± S.E.M.

RESULTS

The experiments described in this paper are based on a total of forty-one TC cells recorded intracellularly from slices of the cat dLGN (lamina A, A1 and C). The passive and active membrane properties of these cells were indistinguishable from those previously reported for TC cells in similar experimental conditions (Leresche *et al.* 1990, 1991). The forty-one cells described in this study include thirty-three (out of 192) neurones which showed rhythmic postsynaptic potentials (i.e. twenty-three with rhythmic EPSPs, including two cells obtained during paired recording; five cells with rhythmic IPSPs; and five cells with rhythmic 'complex potentials') and eight cells that were used for the phase-resetting experiments.

Rhythmic EPSPs

The low-frequency (1·9 ± 0·2 Hz), rhythmic depolarizations were observed in all three laminae of the dLGN and in slices that did or did not contain the perigeniculate nucleus (Figs 1–4). Their amplitude ranged from 1 to 6 mV at resting membrane potential and their duration was 20–60 ms. They occurred rhythmically at a particular frequency (though with the occasional failure of single events), or, in a few

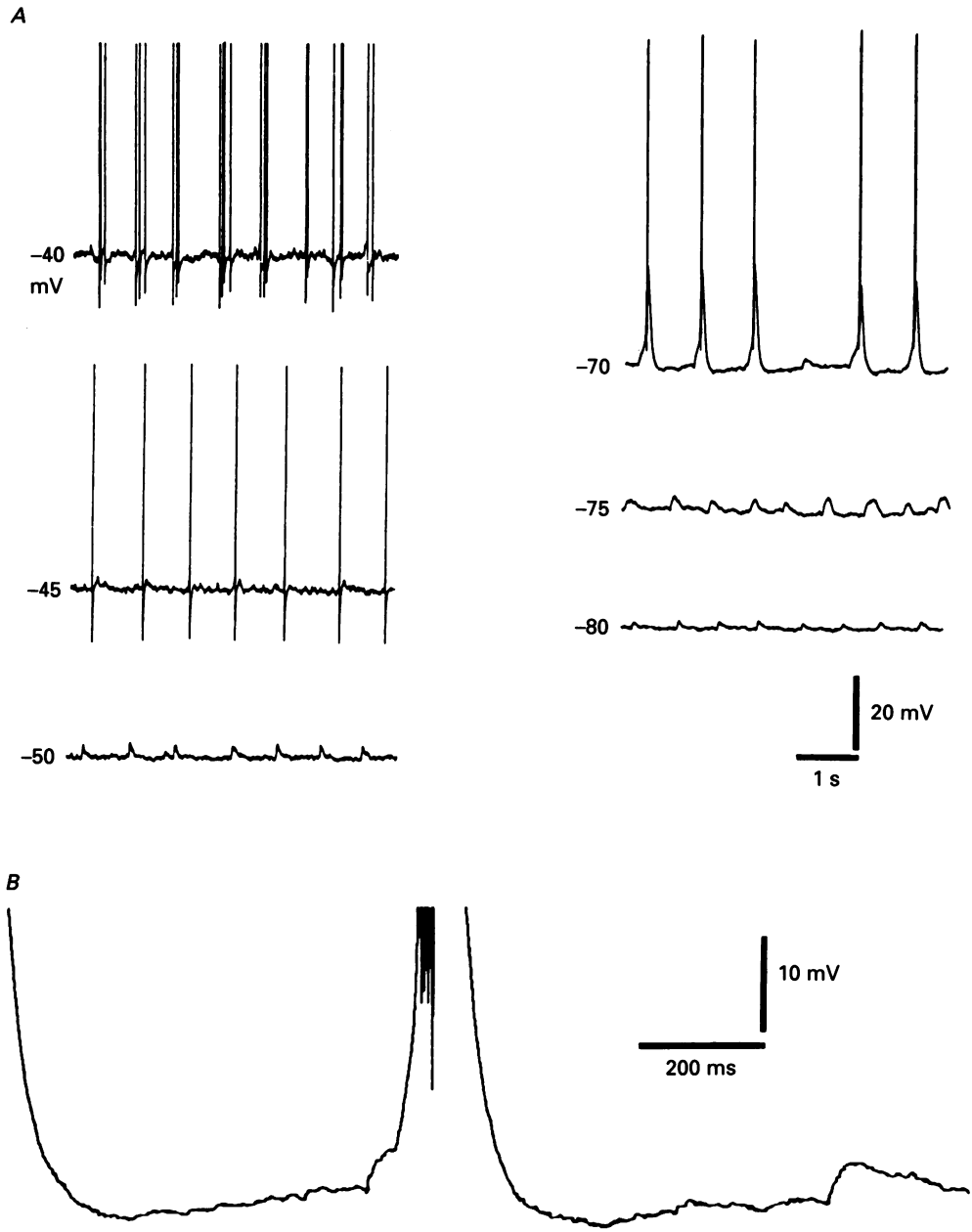

Fig. 1. The low-frequency, rhythmic EPSPs. *A*, intracellular voltage recordings from a TC cell in the cat dLGN shows the rhythmic EPSP recorded at different membrane potentials (obtained by steady current injection). At potentials positive to −50 mV, the EPSPs rhythmically brought the cell to firing threshold. Between −65 and −75 mV, the rhythmic EPSPs could evoke low-threshold Ca^{2+} potentials, while between −50 and −65 mV, or below −75 mV, the EPSPs could be observed in isolation. Note the failure of one of the EPSPs to evoke a low-threshold Ca^{2+} potential in the trace recorded at −70 mV. No major difference in the frequency of the EPSPs was observed at the different membrane potentials. *B*, the middle part of the trace recorded at −70 mV (in *A*) is reproduced at a faster time base in order to show the depolarizing 'hump' (i.e. the EPSP)

cells ($n = 3$), they occurred in periods of activity (5–12 s) interspersed with periods of silence (15–30 s). The frequency of these depolarizations was insensitive to changes in membrane potential obtained by depolarizing and hyperpolarizing current injection (Fig. 1*A*). At membrane potentials positive to −50 mV, they rhythmically evoked action potentials, while between −65 and −80 mV, they could evoke low-threshold Ca^{2+} potentials. At potentials negative to −80 mV, the amplitude of the rhythmic depolarizations decreased, possibly because of the rectification present in these neurones at these membrane potentials (Fig. 1) (Crunelli *et al.* 1987*b*; McCormick & Pape, 1988).

The low-frequency, rhythmic depolarizations were abolished by TTX (0·5–1 μM, $n = 4$) (Fig. 2), suggesting that they were generated either by evoked transmitter release or by a TTX-sensitive, Na^+ current intrinsic to the recorded cell. In order to exclude one of these possibilities, the effect of antagonists selective for excitatory amino acid receptors was also tested. In three cells, simultaneous blockade of NMDA receptors (by 25 μM APV) (Watkins, Krogsgaard-Larsen & Honore, 1990) and non-NMDA receptors (by 10 μM CNQX) (Honore, Davies, Drejer, Fletcher, Jacobsen, Lodge & Neilsen, 1988) abolished the rhythmic depolarizations (Fig. 3), while blockade of $GABA_A$ receptors (by 50 μM bicuculline) had no effect (Fig. 1). These results indicated that the generation of these rhythmic depolarizations involved action potential-driven release of an excitatory amino acid, hence the depolarizations were rhythmic EPSPs.

In some cells, the abolition of the rhythmic EPSPs, either by TTX or by the glutamate antagonists, resulted in the cessation of rhythmic oscillations and associated burst firing, indicating that these TC cells were driven to oscillate by these rhythmic potentials (Fig. 2). Indeed, a closer analysis of these oscillations revealed the lack of a prominent 'pacemaker potential' and the presence of a depolarizing 'hump' (i.e. the EPSP) preceding each low-threshold Ca^{2+} potential (Fig. 1*B*). In other neurones, however, TTX and the glutamate antagonists blocked the EPSPs but not the oscillations, indicating that these cells were genuine intrinsic oscillators (i.e. pacemaker TC cells) (Fig. 3). In the latter cells, once the EPSPs had been abolished, the pacemaker oscillations regained their characteristic rhythm (Fig. 3).

From a total of thirty-two paired intracellular recordings, one pair of TC cells, located about 75 μm apart, displayed simultaneously occurring EPSPs (Fig. 4*A* and *B*). Each rhythmic EPSP in cell 2 was accompanied by a simultaneous EPSP in cell 1, while additional (about 35%) non-concurrent EPSPs were also observed in cell 1. In both cells, at hyperpolarized membrane potentials (< −70 mV) these EPSPs were capable of producing rhythmic low-threshold Ca^{2+} potentials which appeared in a highly phase-locked manner (Fig. 4*C*; see Discussion).

Rhythmic IPSPs

In addition to the rhythmic EPSPs, low-frequency (2·2 ± 0·3 Hz), rhythmic hyperpolarizations were also observed (5 out of 192 cells) in slices that did or did not

immediately preceding the low-threshold Ca^{2+} potential, the absence of a prominent pacemaker potential between successive low-threshold Ca^{2+} potentials, and an EPSP in isolation. This cell was recorded in a slice which did not contain the perigeniculate nucleus, and bicuculline (50 μM) was present in the perfusing medium. In *A*, action potential height has been reduced by the frequency response of the chart recorder.

contain the perigeniculate nucleus (Figs 5 and 6). At −55 mV, the amplitude of these rhythmic hyperpolarizations was 0·5–5 mV and their duration was 15–45 ms. They reversed in polarity at -65 ± 2 mV ($n = 4$) and were abolished by bicuculline (50 μM), indicating that they were $GABA_A$-mediated IPSPs.

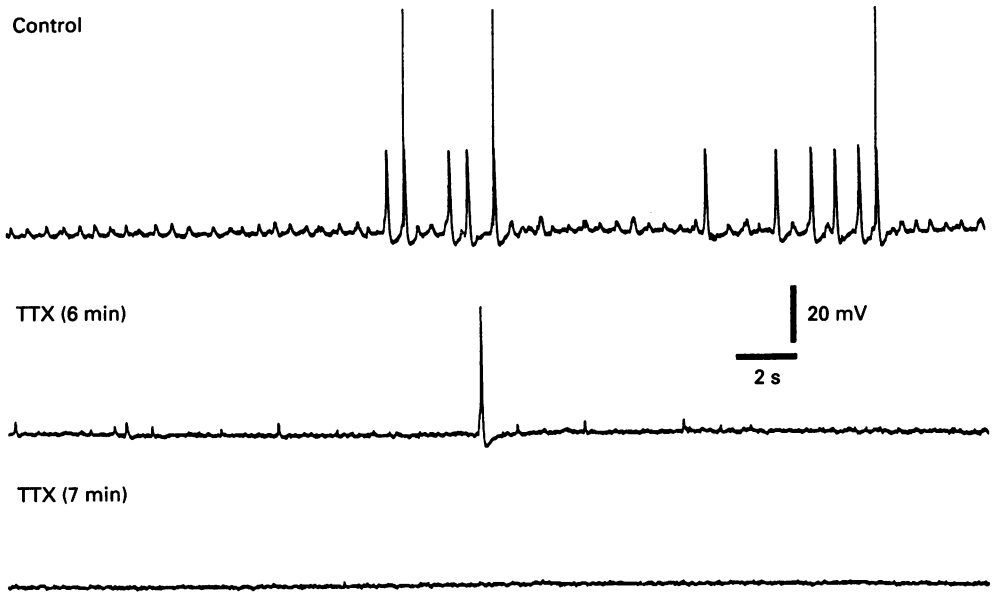

Fig. 2. The effect of TTX on the rhythmic EPSPs. Intracellular voltage records show the rhythmic EPSPs recorded at −70 mV. Some of them were able to evoke a low-threshold Ca^{2+} potential which, in turn, could reach firing threshold. Six minutes after the introduction of a solution containing TTX (0·5 μM), the action potentials were reduced in amplitude and the number of EPSPs drastically reduced. One minute later, the action potentials as well as the rhythmic EPSPs were abolished. In the top trace, action potential height has been reduced by the frequency response of the chart recorder.

At membrane potentials negative to −65 mV and positive to −80 mV, we observed a pattern of activity identical to the one described above for the rhythmic EPSPs, i.e. the depolarizing (i.e. reversed) IPSPs were able to evoke rhythmic low-threshold Ca^{2+} potentials and thus oscillations with associated burst firing (Fig. 5). In these cells, the low-threshold Ca^{2+} potentials were preceded by a depolarizing 'hump' (i.e. the reversed IPSPs) and by a relatively small pacemaker potential (Fig. 5). In contrast, in pacemaker TC cells, bicuculline blocked the IPSPs but not the oscillations (Fig. 6).

Rhythmic, complex synaptic potentials

In addition to rhythmic EPSPs and IPSPs, a complex hyperpolarization–depolarization sequence ('complex potential') was observed in five neurones. These 'complex potentials' occurred rhythmically at a low frequency ($1{\cdot}3 \pm 0{\cdot}3$ Hz) (Fig. 7*A*, Control), were blocked by TTX (0·5 μM; Fig. 7), and were also present in slices that did not include the perigeniculate nucleus. The hyperpolarization (0·5–4 mV at −55 mV) of the 'complex potentials' reversed at -63 ± 3 mV ($n = 5$; Fig. 7), indicating that it was a $GABA_A$-receptor mediated IPSP. The second, depolarizing,

component of the 'complex potentials' had an amplitude of 1–7 mV (measured at 55 mV) and a duration of 40–80 ms.

At potentials positive to −50 mV, the 'complex potentials' evoked a single or a short series of action potentials, while at potentials negative to −65 and positive to

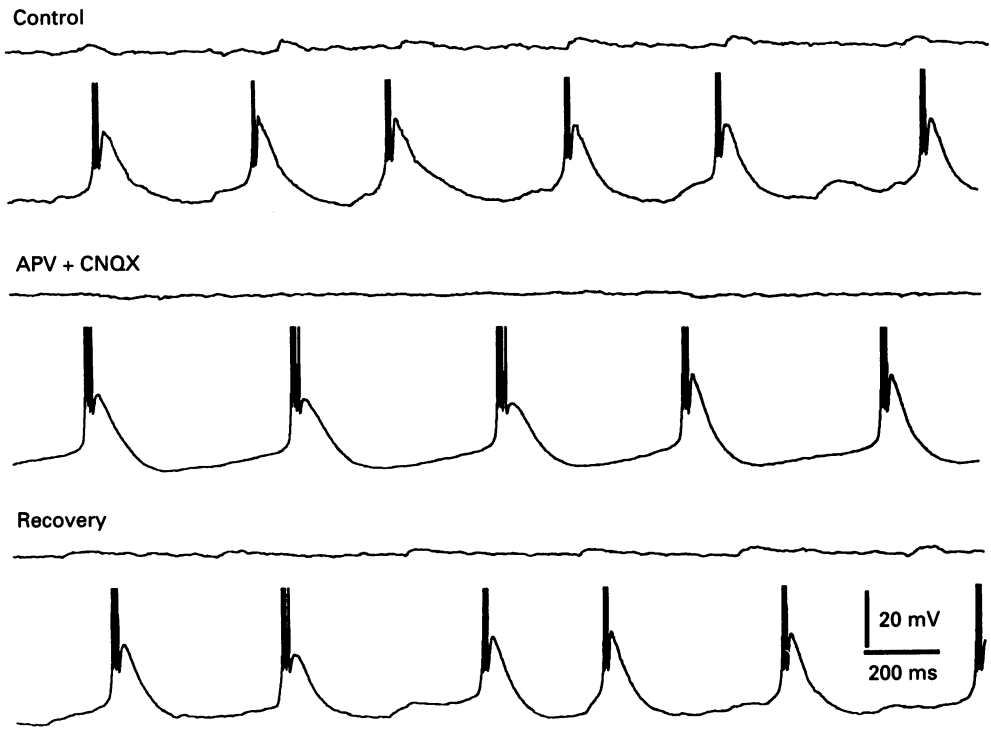

Fig. 3. The effect of APV and CNQX on the rhythmic EPSPs. Intracellular voltage records show the low-frequency, rhythmic EPSPs recorded at −60 mV (Control, top trace) and at −75 mV (Control, bottom trace), where they can still be seen in isolation or as depolarizing 'humps' preceding the low-threshold Ca^{2+} potentials. In the presence of the two excitatory amino acid receptor antagonists APV (25 μM) and CNQX (10 μM) (15 min), the rhythmic EPSPs were abolished (APV+CNQX, top trace, −60 mV), while at a more hyperpolarized membrane potential (APV+CNQX, bottom trace) the cell showed the typical pattern of the pacemaker oscillations (peak of the hyperpolarization: −80 mV). Note the regularity in the frequency of the pacemaker oscillations, when compared to the oscillations recorded in Control. The recovery was obtained 20 min after switching back to the control solution. Action potential height has been reduced by the frequency response of the chart recorder.

−80 mV, they rhythmically evoked low-threshold Ca^{2+} potentials, a pattern of activity similar to the one described above for the rhythmic EPSPs and IPSPs when observed separately (Fig. 7).

Phase resetting experiments

We have described that in pacemaker TC cells the rhythmic synaptic potentials (EPSPs, reversed IPSPs and 'complex potentials') modulated the frequency of the oscillations (Figs 3 and 6). In order to gain insight into the mechanism of phase

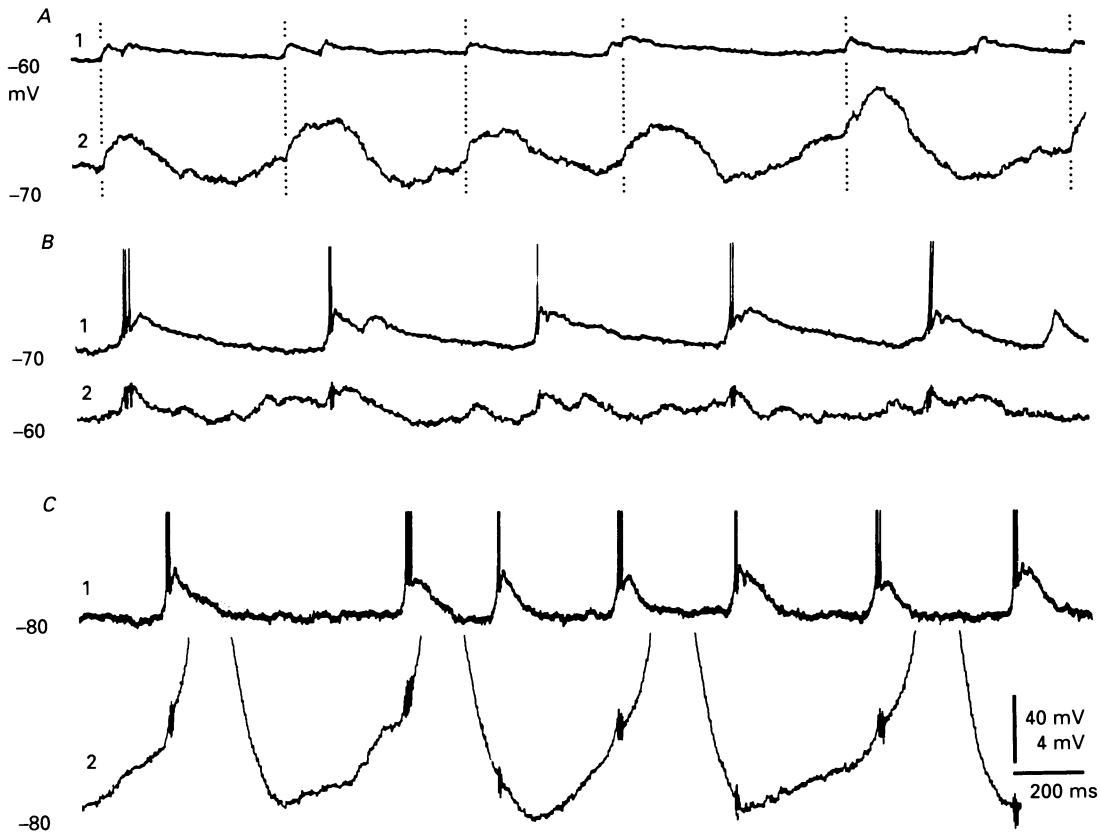

Fig. 4. Rhythmic EPSPs in simultaneously recorded TC cells. Intracellular voltage records were obtained, at the membrane potential shown on the left-hand side of each record, from cell 1 (top trace in *A*, *B* and *C*) and cell 2 (bottom trace in *A*, *B* and *C*) that were located approximately 75 μm apart in a slice that did not contain the perigeniculate nucleus (the upper and lower voltage calibrations refer to the traces of cell 1 and 2, respectively, in *A*, *B* and *C*). *A*, cell 2 displays low-frequency, rhythmic EPSPs, and each time a rhythmic depolarization appears in cell 2, in cell 1 simultaneously occurring depolarizations can be seen, in addition to other, non-concurrent depolarizations. *B*, when cell 1 was hyperpolarized to -70 mV, and cell 2 depolarized to -60 mV, the rhythmic, synchronized EPSPs appeared with unchanged frequency. In cell 1, at this membrane potential, the rhythmic EPSPs evoked low-threshold Ca^{2+} potentials. *C* shows the activity of the two cells when both were hyperpolarized to -80 mV. The EPSPs at this membrane potential evoked low-threshold Ca^{2+} potentials in both cells. The fast voltage deflections in the records obtained from cell 2 in *B* and *C* originate from the action potentials of cell 1, owing to the capacitive coupling between the two intracellular electrodes. There was, however, no voltage response in either of the cells when subthreshold depolarizations were evoked in the other neurone by depolarizing current pulse or by a hyperpolarizing current pulse that triggered a subthreshold, rebound, low-threshold Ca^{2+} potential (not shown). Note also the lack of a concurrent voltage response in cell 2 when cell 1 evokes the last low-threshold Ca^{2+} potential in trace *B* and, vice versa, the lack of a voltage response in cell 1 when cell 2 evokes the low-threshold Ca^{2+} potential in trace *C*. Action potential height in cell 1 has been truncated.

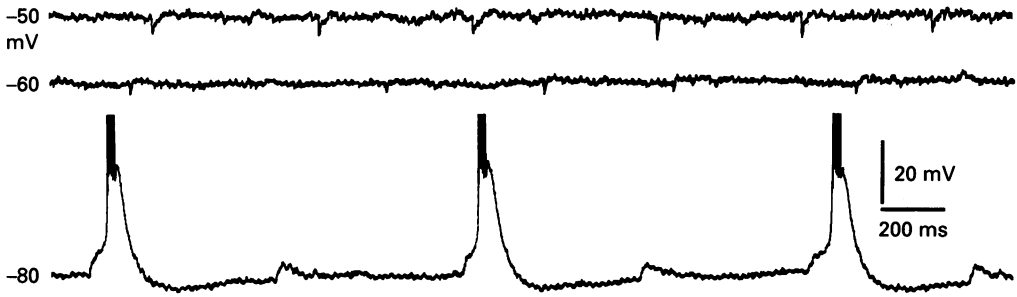

Fig. 5. The low-frequency, rhythmic IPSPs. Intracellular voltage records show the low-frequency, rhythmic IPSPS recorded from a TC cell at three different membrane potentials in a slice that did not contain the perigeniculate nucleus. The IPSPs appeared as hyperpolarizing potentials at −50 and −60 mV, reversed in polarity at −63 mV, and could be observed as depolarizing potentials when the cell was hyperpolarized to potentials more negative than −70 mV. At the latter potentials, the depolarizing IPSPs could be clearly seen in the isolation or as a depolarizing 'hump' immediately preceding the rising phase of the low-threshold Ca^{2+} potentials. Action potential height has been reduced by the frequency response of the chart recorder.

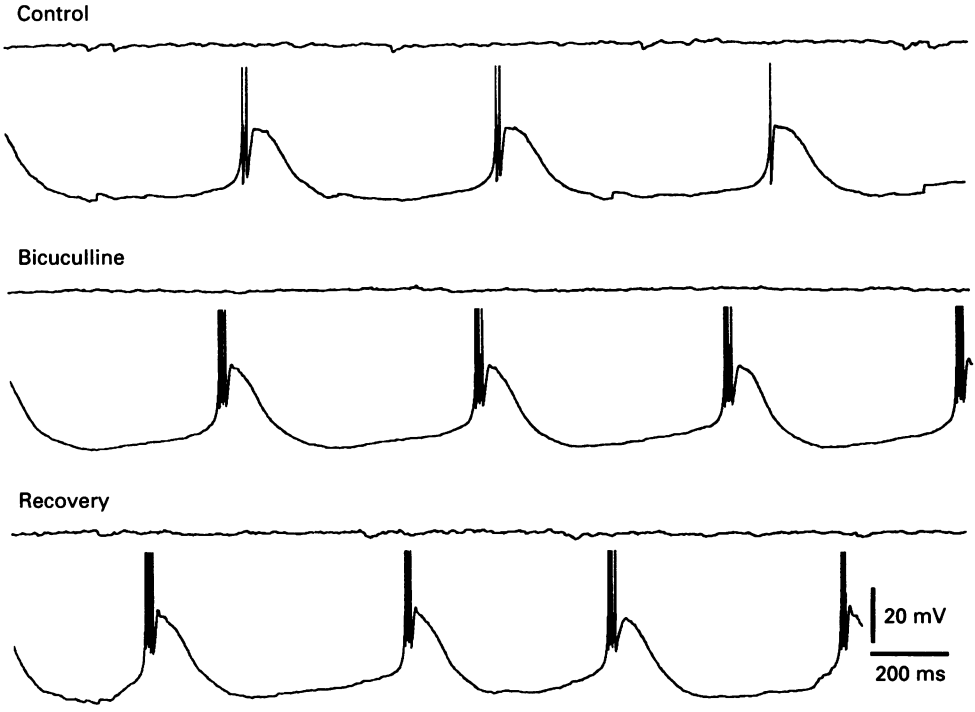

Fig. 6. The effect of bicuculline on the rhythmic IPSPs. Control, intracellular voltage records (obtained from a TC cell in a slice that did not contain the perigeniculate nucleus) shows the low-frequency, rhythmic IPSPs at −55 mV (top trace) and at −75 mV (bottom trace), where they appeared as depolarizing potentials intermixed with low-threshold Ca^{2+} potentials. Eleven minutes after switching to a solution containing bicuculline (50 μM) (Bicuculline), the IPSPs were abolished (−55 mV, top trace), and the cell showed the pattern of activity characteristic of the pacemaker oscillations. Partial recovery was obtained 15 min after switching back to the control solution (Recovery). Action potential height has been truncated.

resettings which might occur during synchronization between TC cells showing pacemaker oscillations, we investigated the effect of single depolarizing current pulses (used to mimic EPSPs and reversed IPSPs) delivered at different phases of the oscillatory cycle. The cells selected for this part of the study either did not show any

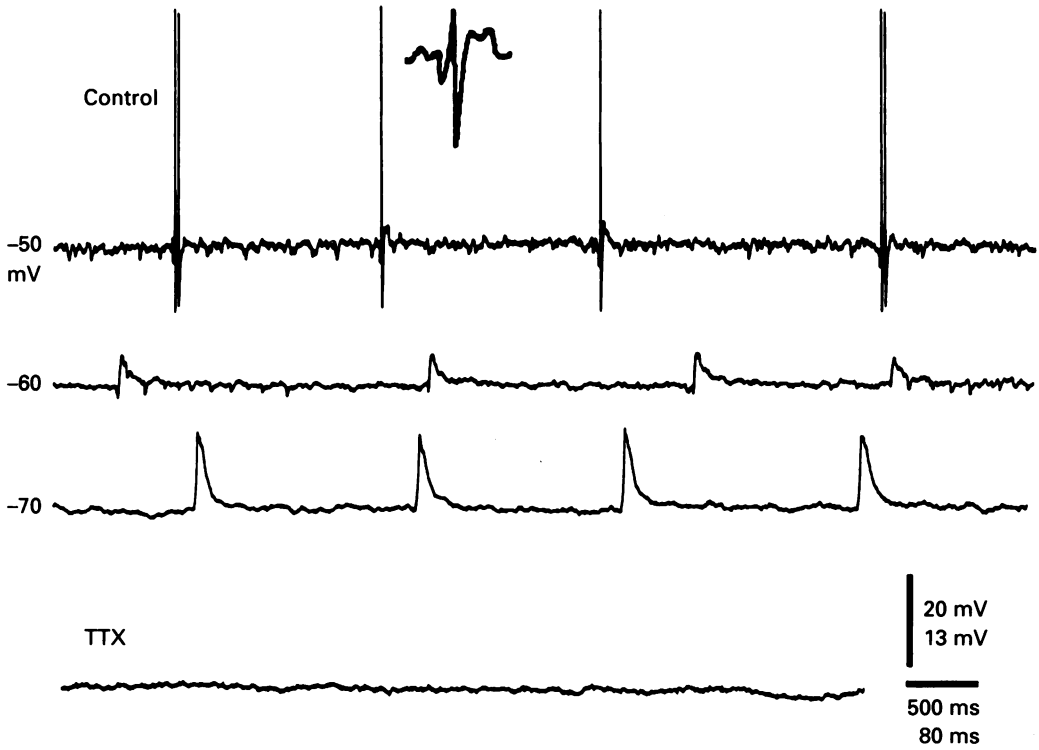

Fig. 7. The voltage dependence of the 'complex potentials' and the effect of TTX. Intracellular voltage records show the IPSP–EPSP sequence of the 'complex potentials' at different membrane potentials. At −50 mV or above, they rhythmically evoked action potential(s). The action potential was preceded by the fast, short-lasting hyperpolarization (see inset above the top trace), which reversed at −65 mV. At −70 mV, the 'complex potentials' began to evoke low-threshold Ca^{2+} potentials. Note that the frequency of the 'complex potentials' was insensitive to changes in the membrane potential. Six minutes after switching to a solution containing TTX (1 μM) the 'complex potentials' were abolished (membrane potential, −50 mV). The lower values for the voltage and time calibration bars refer to the inset. Action potential height has been reduced by the frequency response of the chart recorder.

spontaneous synaptic potentials ($n = 6$; Fig. 9*A–D*) or were recorded in the presence of TTX ($n = 2$; Fig. 9*E*), hence they displayed very stable pacemaker oscillations over a long period of time. Phase-resetting curves (new phase, θ, *versus* old phase, ϕ) were constructed according to the methods developed for the study of other biological oscillators (Winfree, 1970; 1980; Best, 1979; Jalife and Antzelevich, 1979; Guttman, Lewis & Rinzel, 1980; Glass & Mackey, 1988; Jewett, Kronauer & Czeisler, 1991), as explained in Fig. 8.

When the amplitude of the current pulse was relatively large (0·1 nA, 30 ms for the

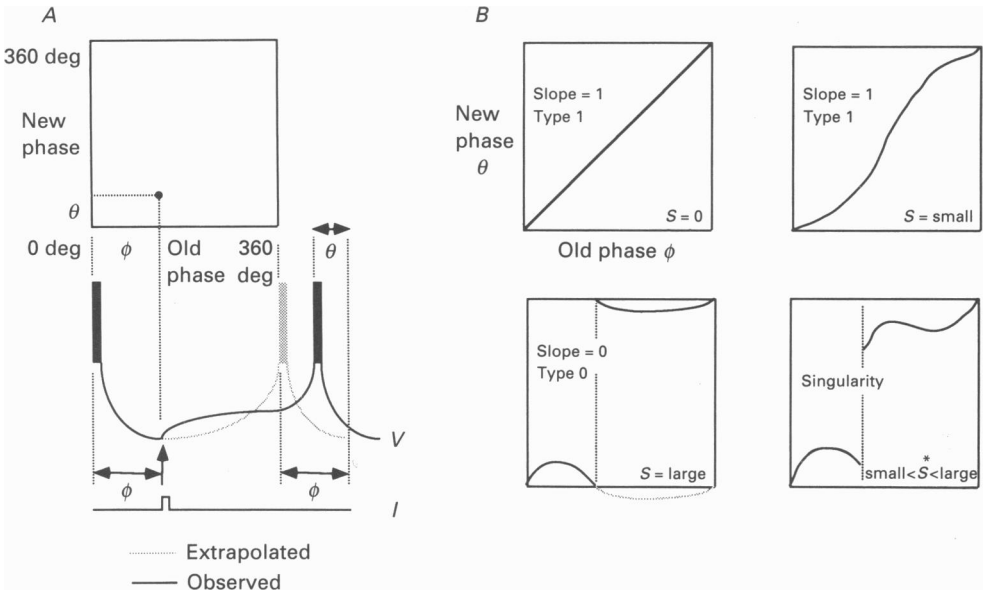

Fig. 8. Construction and types of phase-resetting curves. The phase-resetting curves were generated by perturbing the pacemaker oscillation at different points during its cycle using intracellular injected current pulses that mimicked the EPSPs and the reversed IPSPs. Then the new phase (θ), which the oscillation acquired after the perturbation, with respect to the old phase (ϕ), was recorded (see Winfree, 1970, 1980; Best, 1979; Jalife & Antzelevich, 1979; Guttman *et al.* 1980; Glass & Mackay, 1988; Jewett *et al.* 1991). *A*, shows a schematic representation of the pacemaker oscillations perturbed by a depolarizing current pulse (*I*), 'ϕ' deg after the beginning of the cycle. (Note that the first action potential in a burst was arbitrarily labelled 0 deg phase, the whole cycle being 360 deg). The preperturbation oscillation is then extrapolated and the new phase 'θ' is calculated as shown. This is repeated for several values of 'ϕ' for each transition curve. Then, new curves are generated for several combinations of parameters (i.e. amplitude and duration) of the current pulse. Note that the measurements were taken two or three cycles after the stimulus and not, as shown for clarity in *A*, during the first postperturbation cycle (see Buño, 1984; Glass & Mackay, 1988). *B*, shows examples of type 1 (top plots) and type 0 (bottom plot) resetting curves and the presence of a singularity point. All oscillators can display type 1 resetting since when the perturbing stimulus is zero the new phase equals the old phase, and thus the slope of the resetting curve is 1 (plot marked with $S = 0$). The same applies for small stimuli, for which the average slope of the phase resetting curve is also 1 (plot marked with S = small). In contrast to type 1 resetting, in type 0 resetting the new phase does not cover one complete cycle but only a subset of the possible 0 to 360 deg, hence the two phase-resetting types are qualitatively different. Note that, since 0 deg is no different from 360 deg, the curve in type 0 resetting is a continuous curve, and the apparent discontinuity is only an artifact resulting from the plotting rules (see Glass & Mackay, 1988). This has been highlighted by reproducing the top part of the curve with a dotted curve (plot marked with S = large). When an oscillator displays type 0 resetting there is a singular combination of duration and amplitude of the stimulus (plot marked with S^*) that, when applied at a specific phase, causes unpredictable new phases and can stop the oscillator.

cell shown in Fig. 9*A–D*), we obtained a type 0 resetting curve (Fig. 9*A*). In this case, the relatively large current pulse applied between 0 and 162 deg (0 ms and 268 ms, respectively), caused a progressively longer delay in the appearance of the low-

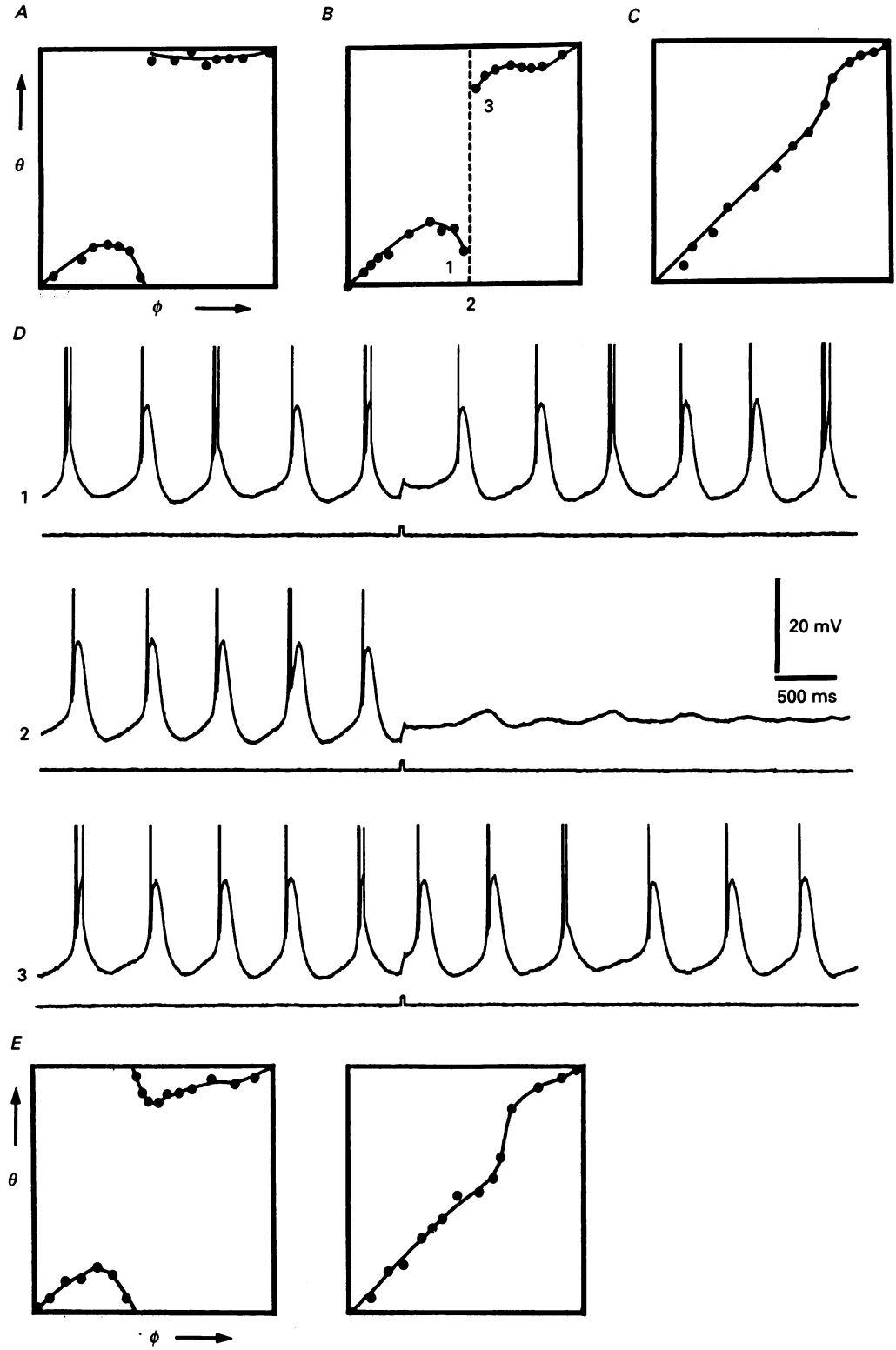

Fig. 9. For legend see facing page.

threshold Ca^{2+} potential, while, when applied between 162 and 360 deg (269 ms and 596 ms) it had the opposite effect. When a current pulse of the same duration (30 ms) but of smaller amplitude (0·01 nA) was used, the new phase increased progressively as the old phase increased: this resulted in a type 1 resetting curve (Fig. 9*C*). The main effect of these small stimuli applied at the late phase of the cycle was that the resulting depolarization caused the first low-threshold Ca^{2+} potential to appear earlier than if the oscillation had not been perturbed.

When an oscillator displays type 0 resetting, there is a singular combination of duration and amplitude of the stimulus that, when applied at a specific phase, causes unpredictable new phases and can stop the oscillator (Winfree, 1970, 1980). For the cell shown in Fig. 9, this singular combination of duration, amplitude and phase was found to be a stimulus of 0·05 nA, with a duration of 30 ms (as above), applied at 186 deg (cycle length: 596 ms; 186 deg: 307 ms) (Fig. 9*B*). When this stimulus was applied slightly before 307 ms (trace 1 in Fig. 9*D*, corresponding to the data point labelled '1' in Fig. 9*B*), it caused the first low-threshold Ca^{2+} potential to appear later. When the stimulus was applied slightly later than 307 ms (trace 3 in Fig. 9*D* corresponding to the data point labelled '3' in Fig. 9*B*), the low-threshold Ca^{2+} potential appeared earlier than it would have done in the absence of the stimulus. However, when the same stimulus was applied at 186 deg, the oscillation stopped (trace 2 in Fig. 9*D*, data point '2' in Fig. 9*B*), until it was restarted by a sufficiently large current pulse.

As shown in Fig. 9*E*, type 0 and type 1 resettings were also obtained by changing the duration of the current pulse while keeping its amplitude constant.

DISCUSSION

The main conclusions of this investigation are (i) that TC cells receive low-frequency, rhythmic EPSPs, IPSPs and 'complex potentials' of intrageniculate origin, (ii) that these TC cells can be either pacemaker cells or cells where the

Fig. 9. Phase-resetting experiments. *A–C*, phase-resetting plots (new phase θ *versus* old phase ϕ) constructed from a TC cell that showed the pacemaker oscillations. The plots were obtained by recording the changes in the phase of poststimulus oscillation with respect to the prestimulus one (see Fig. 8). The stimulus was the depolarizing voltage response obtained by injecting a current pulse of various duration and amplitude through the intracellular electrode. The plot in *A* shows the phase-resetting curve obtained with a current pulse of 0·1 nA (duration: 30 ms) applied at different phases of the cycle. As the old phase was scanned from 0 to 360 deg the new phase did not cover one full cycle, only a subset of the possible 0–360 deg. When a small current pulse (0·01 nA, 30 ms) was used, the new phase covered a full cycle, and the resulting curve had an average slope of 1 (*C*) (i.e. type 1 resetting). When a current pulse of intermediate amplitude was used (0·05 nA, 30 ms), the curve became discontinuous (*B*). *D* shows the three intracellular records (traces 1, 2 and 3) from which the corresponding data points of Fig. 9*B* (labelled 1, 2 and 3, respectively) were obtained. When the current pulse was applied at 186 deg of the cycle (i.e. the point of discontinuity) (trace 2), the oscillation stopped and the new phase became indeterminate. Action potential height has been reduced by the frequency response of the chart recorder. *E* shows type 0 and type 1 phase-resetting plots obtained by changing the duration of the current pulse (left-hand plot: type 0 resetting, 60 ms pulse; right-hand plot: type 1 resetting, 10 ms pulse) while keeping the amplitude constant (0·03 nA). This TC cell was recorded in the presence of TTX (0·5 μM).

oscillations, and the associated burst firing, are induced by the rhythmic synaptic potentials, and (iii) that the effects of a single perturbation on the pacemaker oscillations include phase advance, phase delay or the cessation of the oscillatory activity. Therefore, these results indicate that TC cells in the dLGN could synchronize each other's oscillations and burst firing by intrageniculate mechanisms.

Origin of rhythmic synaptic potentials

EPSPs. The low-frequency, rhythmic EPSPs observed in TC cells of the cat dLGN were blocked by TTX and by the excitatory amino acid receptor antagonists, were insensitive to bicuculline, and were recorded in slices that did not include the perigeniculate nucleus. Furthermore, the mean frequency (1·9 Hz) of the rhythmic EPSPs was similar to one of the pacemaker oscillations (1·8 Hz) (Leresche *et al.* 1990, 1991). Three possibilities can be put forward to explain the origin of these rhythmic synaptic potentials: (i) electrical field effects originating from the pacemaker oscillations of a nearby TC cell or the increase in $[K^+]_o$ associated with the high-frequency burst of action potentials depolarize sensory and cortical terminals that will then produce the rhythmic EPSPs in the recorded cell; (ii) the EPSPs are generated by action potential-driven, rhythmic release of an excitatory amino acid from the severed axon terminals of sensory (i.e. optic tract) and cortical afferents impinging onto the recorded TC cell; (iii) the EPSPs are evoked via axon collaterals of pacemaker TC cells synapsing onto the recorded cell. The first possibility is unlikely since field effects occur mainly in neuronal structures characterized by cellular lamination and high extracellular resistivity (Faber & Korn, 1989) (conditions that do not apply to the dLGN; Jones, 1985), and the increase in $[K^+]_o$ during high-frequency firing (0·2 mM, Sykova, Rothenberg & Krekule, 1974; 2–3 mM, Singer & Lux, 1973) does not seem to be large enough to produce transmitter release. The second possibility cannot be completely excluded at present, although low-frequency, rhythmic, action potential-driven transmitter release from severed axons has not been reported. In addition, low frequency, rhythmic EPSPs, similar to those reported in this paper have been observed *in vivo*, suggesting that they are not artifacts of the slice preparation (Steriade, Curró Dossi & Nunez, 1991*c*; M. Steriade, personal communication). Therefore, the most parsimonious explanation of the origin of the EPSPs is that the pacemaker TC cells rhythmically evoke EPSPs in other oscillating, as well as non-oscillating, TC neurones via intrageniculate collaterals.

Although the number of TC neurones showing collaterals seems to be relatively small (10–15% of the TC cell population; see references in the Introduction), it is possible that their number has been underestimated, since the diameter of these collaterals (0·5 μm) is at the limit of the resolution of the light microscope. In addition, the intrageniculate axon collateral examined in the electron microscope established symmetrical synaptic contacts with dendritic appendages of other TC cells in the cat dLGN (Van Horn *et al.* 1986).

In some TC cells, pacemaker oscillations occur in discrete periods, separated by periods of silence (i.e. the 'spindle-like' oscillations) (see Leresche *et al.* 1990, 1991; Soltesz *et al.* 1991). Interestingly, rhythmic, low-frequency EPSPs which occurred with a similar pattern of activity were recorded from a few TC cells, suggesting that

they could have originated from axon collaterals of neurones which were oscillating in a 'spindle-like' pattern.

IPSPs. The rhythmic IPSPs and 'complex potentials' are also likely to have their origin within the dLGN, since they were recorded in slices that did not contain the perigeniculate nucleus. Thus the rhythmic IPSPs are generated by the dLGN interneurones, which either discharge spontaneously at a low frequency or are under the synaptic influence of pacemaker TC cells. Since geniculate interneurones have not been reported to display pacemaker or other types of low-frequency oscillations (Leresche *et al.* 1991), either a so far undetected population of interneurones exists which can discharge rhythmically at low frequencies, or, more likely, the interneurones are rhythmically driven via intrageniculate collaterals of pacemaker TC cells. The latter possibility is supported by the observation that the synaptic terminals of the collateral studied by Von Horn *et al.* (1986) participated in complex glomeruli.

A similar mechanism to the one described above for the EPSPs and IPSPs might be suggested for the 'complex potentials', i.e. via the same intrageniculate axon collateral of a pacemaker TC cell that innervates an interneurone dendrite as well as the dendritic appendage or dendritic shaft of a TC cell, with the latter postsynaptic to the same interneurone dendrite. The observation that the IPSP preceded the EPSP might be difficult to reconcile with this suggestion. However, a recent study in the anterior thalamic nuclei *in vivo* has indicated that the $GABA_A$, IPSP which is generated in the glomerulus by the interneurone dendrite has a shorter latency than the one which is mediated by the axonal GABA release (Pare, Curró Dossi & Steriade, 1991). Indeed, a similar, short-latency IPSP has been recorded in the dLGN *in vitro* (Soltesz & Crunelli, 1992), sometimes preceding the EPSP (V. Crunelli, unpublished observation).

Synaptic interactions between TC cells

In this study the phase-resetting experiments performed on the *spontaneous* pacemaker oscillations indicated that a single EPSP or a reversed IPSP could not only advance or delay the phase of the oscillations but also abolish them. It is a difficult task to elucidate all the processes underlying these results because of the complex dynamics of the system (see McCormick, Huguenard & Strowbridge, 1991; Toth & Crunelli, 1992*a*). Some indications, however, can be obtained by considering the effect that the perturbing depolarization would have on I_T and I_h, the two voltage-dependent currents that are essential for this type of oscillation (McCormick & Pape, 1990*b*; Soltesz *et al.* 1991). A depolarization below the voltage threshold for the activation of the low-threshold Ca^{2+} potential would decrease the hyperpolarization which activates I_h and de-inactivates I_T, and would therefore delay the appearance of the first poststimulus low-threshold Ca^{2+} potential. A depolarization which arrives after the absolute refractory period of the low-threshold Ca^{2+} potential and which is large enough to reach the voltage threshold for the de-inactivation of I_T, would result in the earlier appearance of the first poststimulus low-threshold Ca^{2+} potential. A depolarization that does not reach the voltage threshold for the activation of the low-threshold Ca^{2+} potential and that arrives at a point in the cycle where its effect on the hyperpolarization necessary for the activation of I_h and the de-

inactivation of I_T is maximal, will annihilate the oscillation, probably because it results in a very slow return of the membrane potential to the voltage threshold for the activation of the low-threshold Ca^{2+} potential. Indeed, computer simulations using a biophysical model that includes only I_T, I_h and a leakage current indicate the presence of a singularity of the membrane conductance near the most hyperpolarized membrane potential reached by the pacemaker oscillations (Toth & Crunelli, 1992*b*). The results of the present study complement a recent investigation on the changes in excitability occurring in TC cells during a synaptically evoked, long-lasting hyperpolarization that produced a rebound low-threshold Ca^{2+} potential (a sequence of membrane potential changes similar to a cycle of spontaneous pacemaker oscillations) (McCormick & Feeser, 1990). These authors have shown that the injection of a depolarizing current pulse at the peak of the hyperpolarization could substantially reduce the amplitude of the rebound low-threshold Ca^{2+} potential.

Functional significance

Recent *in vivo* and *in vitro* studies have demonstrated the presence of low-frequency (0·5–4 Hz), pacemaker oscillations in TC cells, indicating that the EEG oscillations which occur at similar low frequencies (0·5–4 Hz), i.e. the δ-waves, might have thalamic origin (Leresche *et al.* 1990, 1991; McCormick & Pape, 1990*a*, *b*; Soltesz *et al.* 1991; Steriade *et al.* 1991*b*). The mechanisms suggested to synchronize oscillating TC cells have been thought to involve the perigeniculate/reticular thalamic nucleus and the corticothalamic loop (Steriade *et al.* 1991*a*, *b*). The results reported in this paper suggest that the synaptic interactions taking place between TC cells within the dLGN, i.e. in the absence of the perigeniculate/reticular thalamic nucleus and the cortex, might also contribute to the synchronization. Firstly, pacemaker TC cells can drive non-oscillating cells to produce regular membrane potential oscillations and associated burst firing via rhythmic synaptic potentials. Secondly, small amplitude short-lasting depolarizations (mimicking the EPSPs and reversed IPSPs) are capable of abolishing and resetting the phase of the pacemaker oscillations. Thus the rhythmic synaptic potentials provide a means for phase-locking oscillations and burst firing of TC cells.

The effect of an unperturbed oscillator on a pacemaker neurone depends on the strength of the coupling and the intrinsic membrane properties of the neurone. Theoretical calculations have shown that the stabilization of the phase between two oscillations coupled via 'weak' EPSPs occurs gradually through several cycles, with the required number of cycles being inversely proportional to the strength of the excitatory drive (Segundo & Khon, 1981; Buño, 1984). Clearly, two coupled TC cells will not burst in perfect synchrony since there is a time lag between the first action potential in the cell generating the synaptic potential and the first action potential in the burst evoked in the driven cell (due not only to the synaptic delay but also to the relatively slow rise-time of the synaptic potential and of the low-threshold Ca^{2+} potential; see Fig. 1*B*). This time lag between any two coupled cells will also vary continuously owing to small, local changes in extrageniculate synaptic influences which could transiently alter the intrinsic membrane properties of the cell. Thus after each small perturbation a number of cycles will be required for each cell pair to regain the original degree of phase-locking and synchronization, and during this time a new perturbation could also occur. None the less, the rhythmic synaptic potentials will

contribute to the phase-locking of individual oscillators and are therefore likely to exert an overall synchronizing influence, which, together with other synchronizing devices such as the reticular thalamic nucleus and the corticothalamic loop, may contribute to the appearance of slow waves in the EEG. This suggestion is supported by the observation that rhythmic EPSPs occur synchronously in two TC cells, indicating the divergence of the synchronizing input. It should be noted, however, that the synchronization of TC cells observed in this study was facilitated by the removal of disruptive extranuclear influences.

It has been shown that the spontaneous pacemaker oscillations can be blocked by a steady depolarization of the oscillating neurone (Leresche *et al.* 1990, 1991; McCormick & Pape, 1990*a*, *b*), as it occurs *in vivo* as a result of the depolarizing effect produced by extra-thalamic afferents during rapid eye movement sleep and wakefulness (Hirsch *et al.* 1983; Steriade *et al.* 1991*b*). An interesting result of the present study is that the pacemaker oscillations can also be blocked by a single, relatively small and short, depolarization (mimicking an EPSP or a reversed IPSP), provided it arrives at a specific point in the cycle. *In vivo*, such depolarizations might obviously originate not only from within the dLGN, but from an extra-geniculate or extra-thalamic source as well, and they might contribute to the interruption of burst firing in TC cells even in the absence of a steady depolarization of the membrane potential (see Llinas & Yarom, 1986).

Synaptic interactions via intrageniculate collaterals might also occur in the awake state. The three main types of cat dLGN neurones (the X, Y and W cells) possess intrageniculate collaterals (Friedlander *et al.* 1981; Stanford *et al.* 1983; Humphrey & Weller, 1988). Our data suggests that the postsynaptic targets of these collaterals might include interneurones and TC cells, supporting the possibility of complex information processing involving intrageniculate excitatory and inhibitory networks (Andersen & Andersson, 1968; Steriade *et al.* 1990).

We wish to thank Drs L. Glass and R. Miles for their advice on the phase-resetting and paired-recording experiments, respectively, and Drs N. Leresche, S. Lightowler and Z. Emri for their invaluable help in some of the experiments. The work was supported by the Wellcome Trust (grants 17953 and 19135) and by the Central Research Fund of the University of London.

REFERENCES

ANDERSEN, P. & ANDERSSON, S. A. (1968). *Physiological Basis of Alpha Rhythm.* Appleton–Century–Crofts, New York.

BEST, E. N. (1979). Null space in the Hodgkin–Huxley equations. *Biophysical Journal* **27**, 87–104.

BUÑO, T. (1984). Information processing by pacemaker neurons. In *Cortical Integration*, ed. REINOSO-SUAREZ, F. & AJMONE-MARSAN, C. pp. 37–50. Raven Press, New York.

COULTER, D. A., HUGUENARD, J. R. & PRINCE, D. A. (1989). Calcium currents in rat thalamocortical relay neurones: kinetic properties of the transient low-threshold current. *Journal of Physiology* **414**, 587–604.

CRUNELLI, V., KELLY, J. S., LERESCHE, N. & PIRCHIO, M. (1987*a*). The ventral and dorsal lateral geniculate nucleus of the rat: intracellular recordings *in vitro*. *Journal of Physiology* **384**, 587–601.

CRUNELLI, V., LERESCHE, N. & PARNAVELAS, J. G. (1987*b*). Membrane properties of morphologically identified X and Y cells in the lateral geniculate nucleus of the cat *in vitro*. *Journal of Physiology* **390**, 243–256.

CRUNELLI, V., LIGHTOWLER, S. & POLLARD, C. E. (1989). A T-type Ca^{2+} current underlies low-

threshold Ca^{2+} potentials in cells of the cat and rat lateral geniculate nucleus. *Journal of Physiology* **413**, 543–561.

FABER, D. S. & KORN, H. (1989). Electrical field effects: their relevance in central neural networks. *Physiological Reviews* **69**, 821–863.

FRIEDLANDER, M. J., LIN, C. S., STANFORD, L. R. & SHERMAN, S. M. (1981). Morphology of functionally identified neurones in the lateral geniculate nucleus of the cat. *Journal of Neurophysiology* **46**, 80–129.

GLASS, L. & MACKEY, M. C. (1988). *From Clocks to Chaos: The Rhythms of Life*. Princeton University Press, Princetown, NJ, USA.

GUILLERY, R. W. (1966). A study of Golgi preparations from the lateral geniculate nucleus of the adult cat. *Journal of Comparative Neurology* **128**, 21–50.

GUTTMAN, R., LEWIS, S. & RINZEL, J. (1980). Control of repetitive firing in squid axon membrane as a model for a neuronal oscillator. *Journal of Physiology* **305**, 377–395.

HERNANDEZ-CRUZ, A. & PAPE, H.-C. (1989). Identification of two calcium currents in acutely dissociated neurons from the lateral geniculate nucleus. *Journal of Neurophysiology* **61**, 1270–1283.

HIRSCH, J. C., FOURMENT, A. & MARC, M. E. (1983). Sleep-related variations of membrane potential in the lateral geniculate body relay neurons of the cat. *Brain Research* **259**, 308–312.

HONORE, T., DAVIES, S. N., DREJER, J., FLETCHER, E. J., JACOBSEN, P., LODGE, D. & NEILSEN, P. E. (1988). Quinoxalinediones: potent competitive non-NMDA receptor antagonists. *Science* **241**, 701–703.

HUMPHREY, A. L. & WELLER, R. E. (1988). Structural correlates of functionally distinct X-cells in the lateral geniculate nucleus of the cat. *Journal of Comparative Neurology* **268**, 429–447.

JAHNSEN, H. & LLINAS, R. R. (1984). Electrophysiological properties of guinea-pig thalamic neurones; an *in vitro* study. *Journal of Physiology* **349**, 205–226.

JALIFE, J. & ANTZELEVICH, C. (1979). Phase resetting and annihilation of pacemaker activity in cardiac tissue. *Science* **206**, 695–697.

JEWETT, M. E., KRONAUER, R. E. & CZEISLER, C. A. (1991). Light-induced suppression of endogenous circadian amplitude in humans. *Nature* **350**, 59–62.

JONES, E. G. (1985). *The Thalamus*. Plenum Press, New York.

LERESCHE, N., JASSIK-GERSCHENFELD, D., HABY, M., SOLTESZ, I. & CRUNELLI, V. (1990). Pacemaker-like and other types of spontaneous membrane potential oscillations of thalamocortical cells. *Neuroscience Letters* **113**, 72–77.

LERESCHE, N., LIGHTOWLER, S., SOLTESZ, I., JASSIK-GERSCHENFELD, D. & CRUNELLI, V. (1991). Low-frequency oscillatory activities intrinsic to rat and cat thalamocortical cells. *Journal of Physiology* **441**, 155–174.

LLINAS, R. R. & YAROM, Y. (1986). Oscillatory influence of guinea-pig olivary neurones and their pharmacological modulation: an *in vitro* study. *Journal of Physiology* **376**, 163–182.

MCCORMICK, D. A. & FEESER, H. R. (1990). Functional implications of burst firing and single spike activity in lateral geniculate relay neurones. *Neuroscience* **39**, 103–113.

MCCORMICK, D. A., HUGUENARD, J. & STROWBRIDGE, B. W. (1992). Determination of state dependent processing in thalamus by single neuron properties and neuromodulators. In *Single Neuron Computation*, ed. MCKENNA, T., DAVIES, J. & ZORNETZER, S. F. Academic Press, London (in the Press).

MCCORMICK, D. A. & PAPE, H. C. (1988). Acetylcholine inhibits identified interneurons in the cat lateral geniculate nucleus. *Nature* **334**, 246–248.

MCCORMICK, D. A. & PAPE, H. C. (1990*a*). Properties of a hyperpolarization-activated cation current and its role in rhythmic oscillation in thalamic relay neurones. *Journal of Physiology* **431**, 291–318.

MCCORMICK, D. A. & PAPE, H. C. (1990*b*). Noradrenergic and serotoninergic modulation of a hyperpolarization-activated cation current in thalamic relay neurones. *Journal of Physiology* **431**, 319–342.

MCCORMICK, D. A. & PRINCE, D. A. (1987). Actions of acetylcholine in the guinea-pig and cat medial and lateral geniculate nuclei, *in vitro*. *Journal of Physiology* **392**, 147–165.

MADARASZ, M., GERLE, F., HAJDU, F., SOMOGYI, G. & TOMBOL, T. (1978). Quantitative histological studies on the lateral geniculate nucleus in the cat. III. Distribution of different types of neurons in several layers of LGN. *Journal für Hirnforschung* **19**, 193–201.

O'LEARY, J. L. (1940). A structural analysis of the lateral geniculate nucleus of the cat. *Journal of Comparative Neurology* **73**, 405–430.

PARE, D., CURRÓ DOSSI, R. & STERIADE, M. (1991). Three types of inhibitory postsynaptic potentials generated by interneurons in the anterior thalamic complex of the cat. *Journal of Neurophysiology* **66**, 1190–1204.

POLLARD, C. E. & CRUNELLI, V. (1988). Intrinsic membrane currents in projection cells of the cat and rat lateral geniculate nucleus. *Neuroscience Letters Supplement* **32**, S39.

RAMÓN Y CAJAL, S. (1911). *Histologie du Système Nerveux de l'Homme et des Vertebrés*. A. Maloine, Paris.

SCHEIBEL, M. E. & SCHEIBEL, A. B. (1966). Patterns of organization in specific and non-specific thalamic fields. In *The Thalamus*, ed. PURPURA, D. P. & YAHR, M. D., pp. 13–46. Columbia University Press, New York.

SEGUNDO, J. P. & KHON, A. F. (1981). A model of excitatory synaptic interactions between pacemakers. Its reality, its generality, and the principles involved. *Biological Cybernetics* **40**, 113–126.

SINGER, W. & LUX, H. D. (1973). Presynaptic depolarization and extracellular potassium in the cat lateral geniculate nucleus. *Brain Research* **64**, 17–33.

SOLTESZ, I. & CRUNELLI, V. (1991). Coupling of neuronal oscillators *via* intranuclear collaterals in the dorsal lateral geniculate nucleus (dLGN). *Society for Neuroscience Abstracts* **17**, 282.10.

SOLTESZ, I. & CRUNELLI, V. (1992). $GABA_A$ and pre- and post-synaptic $GABA_B$ receptor-mediated responses in the lateral geniculate nucleus. In *GABA in the Retina and Central Visual System*, ed. MIZE, R. R., MARC, R. & SILLITO, A. M. pp. 151–169. Elsevier, Amsterdam.

SOLTESZ, I., LIGHTOWLER, S., LERESCHE, N., JASSIK-GERSCHENFELD, D., POLLARD., C. E. & CRUNELLI, V. (1991). Two inward currents and the transformation of low-frequency oscillations of rat and cat thalamocortical cells. *Journal of Physiology* **441**, 175–197.

STANFORD, L. R., FRIEDLANDER, M. J. & SHERMAN, S. M. (1983). Morphological and physiological properties of geniculate W-cells of the cat: a comparison with X- and Y-cells. *Journal of Neurophysiology* **50**, 582–608.

STERIADE, M., CURRÓ DOSSI, R. & NUNEZ, A. (1991*a*). Intracellular studies of thalamic neurons generating sleep delta waves and fast (40 Hz) oscillations during arousal. In *Basic Mechanisms of the EEG*, ed. ZSCHOCKE, S. & SPECKMAN, E. J., Birkhauser, Boston (in the Press).

STERIADE, M., CURRÓ DOSSI, R. & NUNEZ, A. (1991*b*). Network modulation of a slow intrinsic oscillation of cat thalamocortical neurons implicated in sleep delta waves: cortical potentiation and brainstem cholinergic suppression. *Journal of Neuroscience* **11**, 3200–3218.

STERIADE, M., CURRÓ DOSSI, R. & NUNEZ, A. (1991*c*). Network modulation of an intrinsic delta (0·5–4 Hz) rhythm in thalamic neurons. *Society for Neuroscience Abstracts* **17**, 631.3.

STERIADE, M., JONES, E. G. & LLINAS, R. R. (1990). *Thalamic Oscillations and Signaling*. J. Wiley & Sons, New York.

SUZUKI, S. & ROGAWSKI, M. A. (1989). T-type calcium channels mediate the transition between tonic and phasic firing in thalamic neurons. *Proceedings of the National Academy of Sciences of the USA* **86**, 7228–7232.

SYKOVA, E., ROTHENBERG, S. & KREKULE, I. (1974). Changes of extracellular potassium concentration during spontaneous activity in the mesencephalic reticular formation of the rat. *Brain Research* **79**, 333–337.

TOMBOL, T. (1967). Short neurons and their synaptic relations in specific thalamic nuclei. *Brain Research* **3**, 307–326.

TOMBOL, T., MADARASZ, M., HAJDU, F., SOMOGYI, G. & GERLE, J. (1978). Quantitative studies on the lateral geniculate nucleus in the cat. I. Measurement on Golgi material. *Journal für Hirnforschung* **19**, 145–158.

TOTH, T. & CRUNELLI, V. (1992a). Computer simulation of the pacemaker oscillations of thalamocortical cells. *Neuroreport* **3**, 65–68.

TOTH, T. & CRUNELLI, V. (1992*b*). Modelling of pacemaker oscillations in thalamocortical neurones. In *Cybernetics and System '92*, ed. TRAPPI, R., pp. 749–756. World Scientific Publishing Co., Singapore.

VON HORN, S. C., HAMOS, J. E. & SHERMAN, S. M. (1986). Ultrastructure of the intrageniculate axon collateral of a projection neuron in the cat. *Society for Neuroscience Abstracts* **12**, 285.9.

WATKINS, J. C., KROGSGAARD-LARSEN, P. & HONORE, T. (1990). Structure–activity relationships in the development of excitatory amino acid receptor agonists and competitive antagonists. *Trends in Pharmacological Sciences* **11**, 25–33.

WINFREE, A. T. (1970). An integrated view of the resetting of a circadian clock. *Journal of Theoretical Biology* **28**, 327–374.

WINFREE, A. T. (1980). *The Geometry of Biological Time*. Springer-Verlag Inc, New York.